Current Research (2026) Newfoundland and Labrador Department of Energy and Mines Geological Survey, Report 26-1, pages 255-274

PETROGRAPHY AND GEOCHEMISTRY OF ULTRAMAFIC–MAFIC ROCKS OF THE FLORENCE LAKE GROUP IN THE BAIKIE SUB-BELT, HOPEDALE BLOCK, LABRADOR

M. Schofield, D. Diekrup[1] and S. Serna Ortiz[2]
Mineral Deposits Section
[1]Regional Geology Section
[2]Vale Base Metals

ABSTRACT

The ultramafic and mafic rocks of the Florence Lake Group in the Hopedale Block of northeastern Labrador have long been known to be prospective for Ni mineralization. However, a stratigraphic framework to put the mineralization into context and correlate units between the sub-belts is lacking. Komatiite associated Ni–Cu–PGE deposits are stratiform or stratabound deposits that have a strong volcanic control on their distribution, therefore detailed geological mapping and a proper stratigraphic framework is crucial for successful exploration campaigns.

Sporadic base-metal exploration activity over the past 65 years has mostly focused on the Baikie sub-belt, an 11-km long, 2-km wide, arcuate belt of supracrustal rocks of the Florence Lake Group that hosts 6 Ni–Cu (Co, PGE) prospects along an 8-km strike length of ultramafic and mafic rocks. The highest Ni grades reported were 2.19% Ni, 0.2% Cu and 0.2% Co over an interval of 11 m. The availability of drillcore along with relatively high surface sampling density allows for an extensive dataset to evaluate the stratigraphic controls on mineralization in the Baikie sub-belt and create a foundation for comparison to the rest of the Florence Lake Group. The stratigraphy in the Baikie sub-belt consists of a western domain of dominantly primitive basaltic compositions, and an eastern domain with a general progression up succession, assuming a southeasternly younging direction, from more enriched and contaminated to more depleted and primitive basaltic compositions, along with a concomitant change in chemistry of the ultramafic rocks from Al-depleted to Al-undepleted komatiite. The Ni prospects are hosted by Al-undepleted komatiite units and occur between two compositionally distinct basalt groups in the eastern domain. The mineralized komatiitic rocks show evidence for crustal contamination, including negative Nb, Ta and Ti anomalies and enrichment in highly incompatible lithophile elements. Additionally, the sulphide mineralogy varies as a function of strain and alteration intensity, ranging from relatively undeformed sulphide blebs with intergrown pyrrhotite, pentlandite and chalcopyrite ± pyrite, to highly flattened sulphide blebs with intergrown siegenite, millerite, polydymite, and chalcopyrite with recrystallized euhedral pyrite. Precious-metal and platinum-group-element inclusions in recrystallized pyrite suggests liberation of platinum-group elements from other sulphide phases as well as possible introduction of gold and silver from orogenic fluids during deformation. In addition, the change from pentlandite to more Ni-rich phases (millerite, polydymite) in the more strained and altered Ni-prospects likely have important metallurgical implications. These criteria can be used to look for comparable sequences, and evidence of similar ore-forming processes, in the other sub-belts of the Florence Lake Group.

INTRODUCTION

Archean greenstone belts are major sources of base and precious metals globally (*e.g.*, Abitibi greenstone belt, Ontario and Québec, Canada; Dubé and Mercier-Langevin, 2020; Agnew-Wiluna greenstone belt, Western Australia; Fiorentini *et al.*, 2012) and, importantly, 22 of Canada's 34 critical minerals can be found in deposits associated with greenstone belts (*e.g.*, volcanogenic massive sulphide, and komatiite associated Ni–Cu–Co–PGE deposits). Previous work in the Florence Lake greenstone belt has highlighted the presence of these mineralization styles within the belt (*e.g.*, Brace and Wilton, 1990; Miller, 1996; Figure 1). The highest reported Ni grades in the Florence Lake greenstone belt came from the komatiite associated Baikie prospect with 2.19% Ni, 0.22% Cu and 0.16% Co over 11.3 m of disseminated sulphide mineralization (McLean *et al.*, 1992), including two intervals of massive sulphide with 10.6% Ni, 0.22% Cu, 0.29% Co, 0.52 g/t Pt and 1.64 g/t Pd over 0.9 m and 9.81% Ni, 0.11% Cu, 0.25% Co, 0.15 g/t Pt and 1.52 g/t Pd over 0.5 m (McLean *et al.*, 1992). Additionally, there are several gold occurrences throughout the belt, which are also

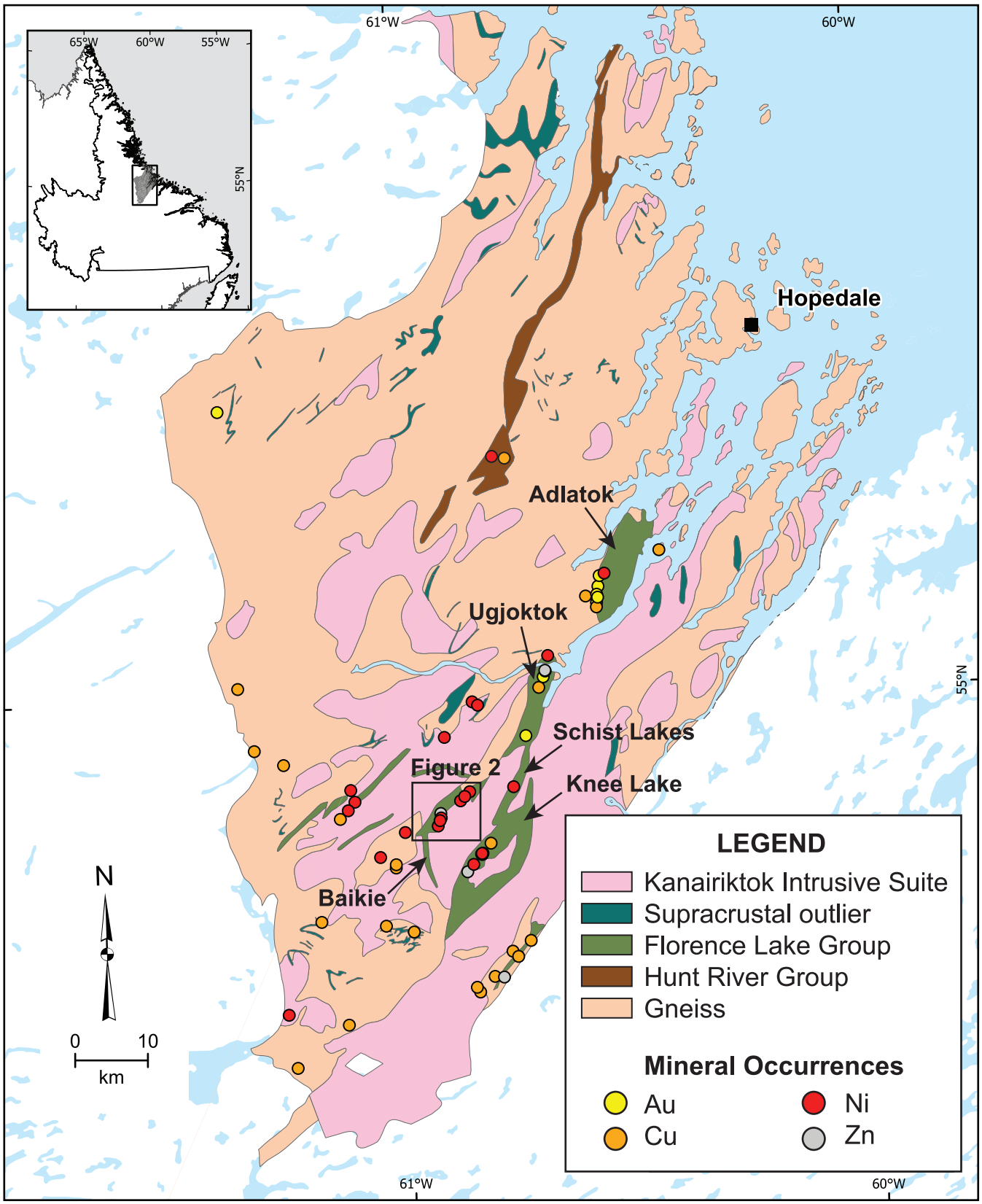

Figure 1. *Simplified geological map of the Hopedale Block showing the distribution of the Florence Lake and Hunt River greenstone belts (modified from Diekrup* et al.*, 2024). Geology after Ermanovics (1993) and Wardle* et al. *(1997). Sub-belts of the Florence Lake greenstone belt are labelled.*

spatially associated with the komatiite units; the highest reported grades are from the TD-500 prospect in the Adlatok sub-belt, with recent channel sampling results of 4.23 g/t Au over 5.04 m (Dunsworth and Moss, 2026).

Presently, however, a belt-wide cohesive structural–stratigraphic framework is lacking, which is essential for targeting these deposits and properly evaluating the mineral potential of the belt. One of the most important aspects of base-metal exploration in volcanic terranes is the recognition of distinct rock types and facies that form markers for economically significant minerals. Metasomatism and deformation, ubiquitous in Archean greenstone belts, obscure primary features critical for the identification of rock type and facies. However, whole-rock chemistry can be used to define a chemostratigraphic framework and provide insight into the geodynamic evolution of greenstone belts and prospectivity for mineralization.

The current study focuses on the petrography and geochemistry of ultramafic and mafic rocks of the Baikie sub-belt (Figure 2) and implications for magmatic Ni-Cu (Co, PGE) potential. This forms part of a broader study investigating the critical-mineral potential within the supracrustal sequences of the Hopedale Block. New data were combined with non-confidential mineral-industry data from assess-

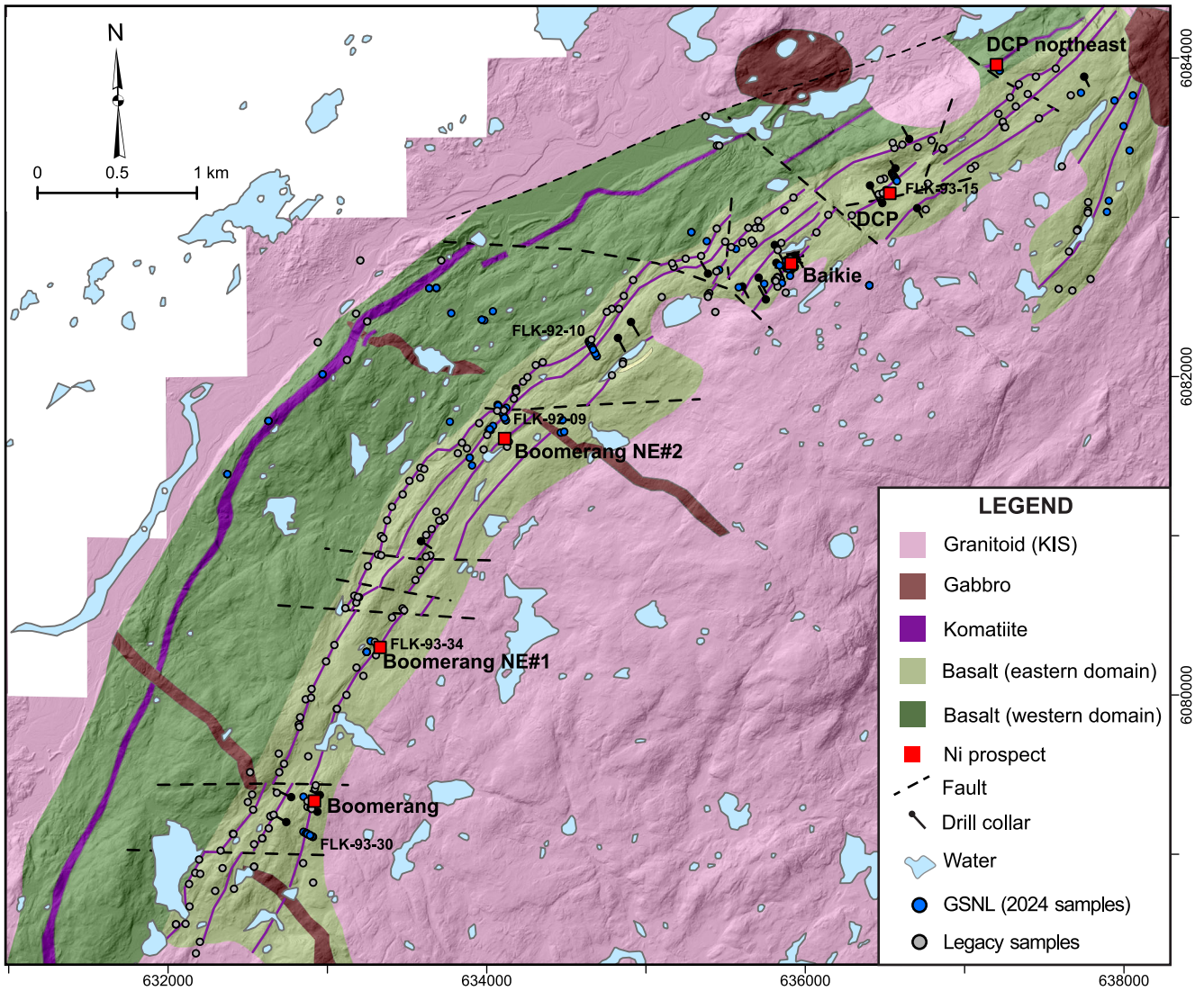

Figure 2. *Local geological map of the Baikie sub-belt (modified from Miller and James, 1997) showing the distribution of known mineral occurrences, legacy samples (McLean* et al.*, 1992; McLean and Butler, 1993)and drillhole traces for holes that were drilled by Falconbridge (McLean* et al.*, 1992; McLean and Butler, 1993) and Tapestry Ventures Limited (Cullen and Churchill, 1997). Diamond-drill holes that were relogged during the present study are labelled. Faults are interpreted using data from available geophysical surveys (Evans-Lamswood and Sobie, 2022), topographic lineaments and/or local surface exposure.*

ment files, resulting in a total dataset of 368 samples. These data are evaluated and discussed in the context of known komatiite associated Ni–Cu (Co, PGE) systems globally, and provide a baseline for comparison to the rest of the belt and other supracrustal sequences within the Hopedale Block. Geochemical results for additional samples collected during the 2025 field season were not available at the time of writing, are not included in this report and will be released at a later date.

REGIONAL GEOLOGY

The Hopedale Block (Figure 1) is a Meso- to Neoarchean granite–greenstone terrane that comprises the southern part of the North Atlantic Craton and is bound by the Paleoproterozoic Makkovik and Torngat orogens to the southeast and west, respectively (Bridgewater *et al.*, 1973; James *et al.*, 2002). The Hopedale Block contains two main supracrustal belts, the *ca.* 3.1 Ga Hunt River Group (HRG) and the *ca.* 3.0 Ga Florence Lake Group (FLG), as well as numerous smaller, coeval and possibly older (>3.2 Ga) supracrustal belt outliers, surrounded by orthogneiss and granitoid intrusions (Sandeman *et al.*, 2023; Hinchey *et al.*, 2024).

The FLG is composed of supracrustal rocks that were deposited between 3003 and 2979 Ma (Ermanovics, 1993; James *et al.*, 2002). It consists predominantly of mafic volcanic rocks, lesser ultramafic and felsic volcanic and volcaniclastic rocks and minor sedimentary rocks (James *et al.*, 2002), which are structurally dismembered into five lenticular, northeast-striking sub-belts termed the Adlatok, Ugjoktok, Baikie, Schist Lakes and Knee Lake (Figure 1; James *et al.*, 1996). The Baikie sub-belt has been subdivided into a western and eastern domain (Miller and James, 1997; Figure 2), based on rock type, magnetic signatures and geochemistry, however, the relationship between the two domains, whether stratigraphic or structural, is uncertain. The *ca.* 2892–2832 Ma Kanairiktok Intrusive Suite (KIS) surrounds and intrudes the volcanic strata of the FLG (Hinchey *et al.*, 2024). Lower amphibolite facies conditions were reached in the contact metamorphic aureole of these younger intrusions, which were overprinted and retrograde metamorphosed by regional greenschist-facies metamorphism and deformation (McLean *et al.*, 1992; Ermanovics, 1993; James *et al.*, 2002). Although all rock types have been metamorphosed, the prefix meta- is omitted in this report for brevity. The volcanic rocks of the FLG were deformed and metamorphosed during a minimum of two deformational events (Diekrup *et al.*, 2023; Schofield and Diekrup, 2025). The first deformation event is characterized by a penetrative sub-vertical, north-northeast striking foliation marked by regional greenschist-facies minerals. Isoclinal folding (F_1) of primary bedding occurs locally with north-northeast striking axial planes (James *et al.*, 1996). The second deformation event is characterized by a spaced north-northwest to south-southeast striking cleavage and open to tight F_2 folds, which overprint S_1 and F_1 (Diekrup *et al.*, 2023, 2024).

PETROGRAPHY

MAFIC ROCKS

The mafic volcanic rocks are typically aphanitic to fine-grained, and moderately to strongly foliated. They are more resistant to weathering than the intercalated ultramafic units and form relative topographic highs. Primary textures, including pillow selvedges and amygdales are observed locally. However, massive flow facies dominate. The mineralogy of the mafic volcanic rocks consists dominantly of hornblende ± actinolite, with lesser quartz, epidote, biotite, chlorite, carbonate and rutile (Plate 1A). Thin intervals of mafic tuff and argillite are locally intercalated with the volcanic flows. The mafic tuff units are fine-grained and have similar mineralogy and chemistry to the mafic volcanic rocks, but are identified as clastic by the presence of compositional banding and grain size variation. The mafic tuff units are typically strongly foliated parallel to bedding and no primary features such as grading or juvenile clasts (*e.g.*, scoria) have been observed. They are classified as tuff following the granulometric classification scheme of Fisher and Schmincke (1984) with no genetic implications for the mode of fragmentation and deposition.

In addition, there are several mafic intrusive phases within the Baikie sub-belt: fine- to medium-grained diabase dykes and medium- to coarse-grained gabbroic dykes and plutons. The diabase dykes strike east to east-northeast are weakly to non-magnetic, and weakly deformed. They weather light-grey and have dark-grey fresh surfaces. They have sharp chilled margins with the volcanic host rocks and are crosscut by granitoid rocks of the KIS. They are glomeroporphyritic consisting of ~2% feldspar glomerocrysts (2–5 mm diameter) in a fine-grained ophitic groundmass defined by randomly oriented feldspar laths enclosed in clinopyroxene oikocrysts. Where the diabase dykes are cut by granitoid rocks of the KIS the clinopyroxene is replaced by granoblastic hornblende. The feldspar in the groundmass and glomerocrysts is heavily saussuritized. Very fine-grained trace ilmenite is present in virtually all diabase samples. Very fine-grained, disseminated pyrite, chalcopyrite, pyrrhotite and pentlandite are also present locally.

Gabbroic dykes strike north-northwest, are strongly magnetic and undeformed. They weather brown and form topographic ridges. The dykes contain 3–5% disseminated fine-grained (~1 mm) magnetite. They are characterized by subophitic texture, with ~20% medium-grained (3–5 mm)

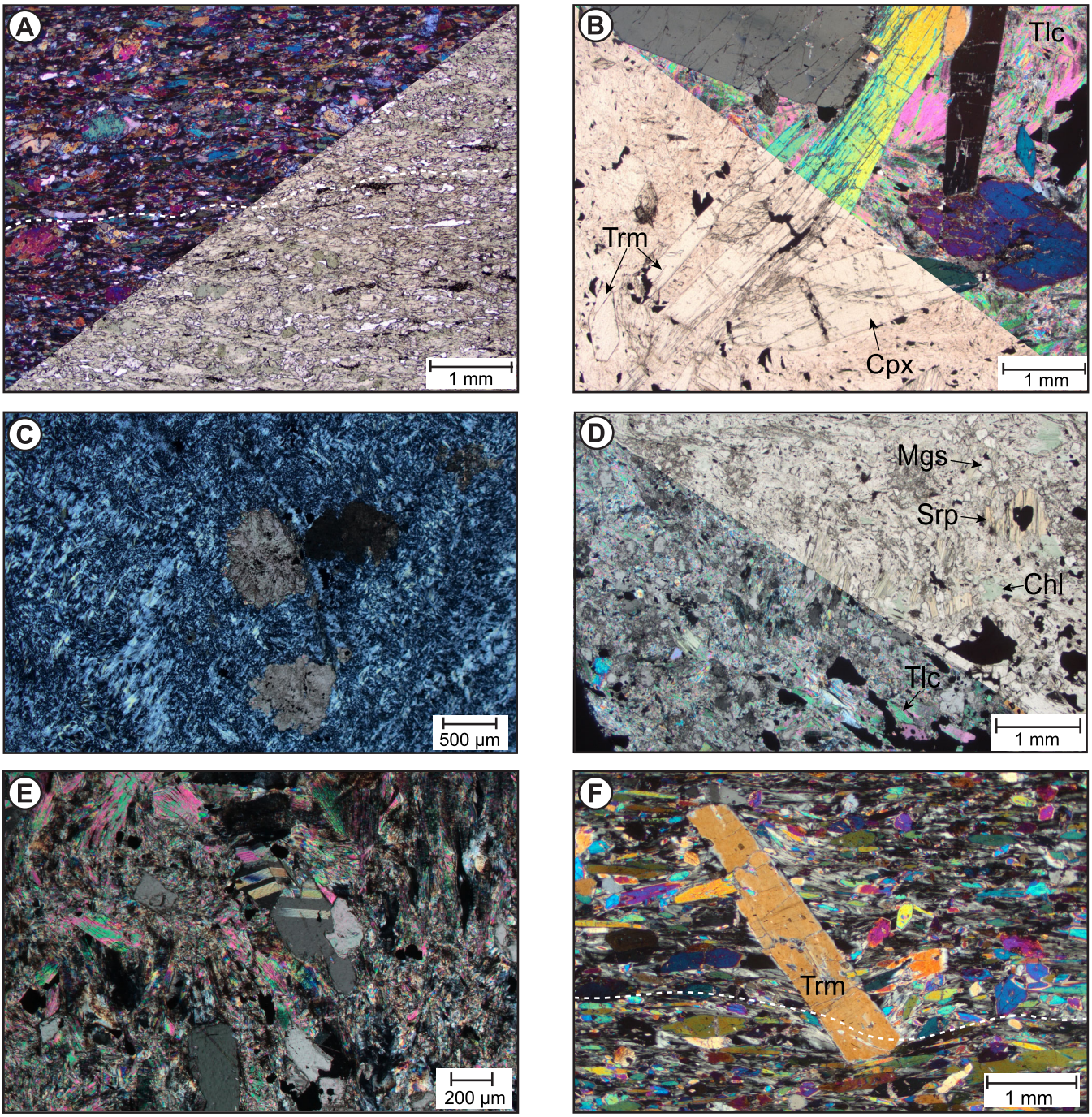

Plate 1. *Photomicrographs showing textures and mineralogy of mafic and ultramafic samples of the Florence Lake Group. A) Sample 24MS0002A, showing moderately foliated basalt. Cross-polarized (top left) and plane-polarized light (bottom right); B) Sample 24MS0001M showing preserved clinopyroxene crystals weakly replaced by talc and carbonate, as well as coarse-grained tremolite. The groundmass is completely replaced by talc. Cross polarized (top right) and plane polarized (bottom left); C) Sample 24MS0139G showing serpentinite with minor fine-grained dolomite crystals. Cross polarized; D) Sample 24MS0001J1 showing talc magnesite altered ultramafic. Cross-polarized (bottom left) and plane-polarized (top right) light; E) Sample 24MS0001J1 showing talc–magnesite altered ultramafic. Cross polarized; F) Sample 24MS0001G1 showing serpentine–tremolite alteration and syn-kinematic coarse-grained tremolite porphyroblasts, with rotated inclusion trail. Cross polarized. Chl–chlorite, Cpx–clinopyroxene, Mgs–magnesite, Srp–serpentine, Trm–tremolite, Tlc–talc.*

euhedral feldspar laths partially enclosed by clinopyroxene. The feldspar laths are saussuritized. Minor (~3%) fine-grained (~200 µm–1 mm) subhedral olivine grains are also present, which are typically crosscut by abundant fractures and variably altered to serpentine.

ULTRAMAFIC ROCKS

Primary minerals are typically not preserved in the ultramafic rocks of the FLG, because of overprinting metasomatism and deformation. However, clinopyroxene is rarely preserved in serpentine- or talc-altered rocks with minimal to no carbonate (Plate 1B). There are five secondary mineral associations observed in the ultramafic rocks of the FLG: 1) serpentine (± carbonate) (Plate 1C), 2) talc–magnesite (± dolomite) (Plate 1D, E), 3) actinolite–tremolite (± chlorite, talc) (Plate 1F), 4) biotite–hornblende, and 5) magnesite–quartz (± dolomite, ankerite). The term mineral association refers to alteration or metamorphic minerals that occur together and characterize a distinct alteration type but may not be in equilibrium or have formed at the same time (Einaudi *et al.*, 2003).

Serpentine (± carbonate) is the earliest mineral association and is related to early seafloor hydration reactions of primary ultramafic minerals (olivine, pyroxene) forming serpentine and magnetite. Serpentine occurs as thin fibrous veinlets and fine-grained aggregates, associated with fine-grained magnetite (Plate 1C). Locally, fine-grained (0.5–1 mm) carbonate crystals overgrow the earlier serpentine and magnetite. Serpentinized rocks represent the least altered rocks in the FLG and are relatively rare.

The most abundant association is talc–magnesite (Plate 2A), interpreted to have formed during regional metamorphism, wherein the pre-existing serpentinites reacted with CO_2- and SiO_2-rich fluids; magnesite is the dominant carbonate phase, but it is progressively replaced by dolomite and ankerite in proximity to later shear zones. Modal chlorite also appears to increase with increased strain and a concomitant decrease in talc abundance (Plate 2B, C).

The actinolite–tremolite (± chlorite, talc) and biotite–hornblende associations are spatially associated with the KIS, typically have gradational contacts and show decussate texture indicating that these mineral associations are related to contact metamorphism. Locally, coarse-grained tremolite porphyroblasts show rotated inclusion trails that align with the main pervasive northeast striking foliation (Plate 1F), suggesting that they grew syn-deformation.

The most intense alteration involves almost complete replacement of silicate phases by magnesite (± ankerite ± dolomite) and quartz (Plate 3A–C). This last alteration association contains only trace magnetite; the carbonate phases likely incorporated the iron formerly in magnetite. This is supported by the lack of magnetite in carbonate-rich domains compared to chlorite-rich domains in the thin section (Plate 2B) and the general decrease in magnetite modal abundances with increasing carbonate. Because of the magnetite destructive nature of this alteration, the rock's magnetic signal is reduced, which results in localized mag-lows in the regional geophysical surveys. The carbonatization of talc ± serpentine-rich rocks increases the mechanical strength of the rock leading to more brittle deformation styles and an increased abundance of quartz-carbonate veining, which have the potential to host orogenic gold mineralization (*e.g.*, Thurber Dog, Adlatok sub-belt; Figure 1). Furthermore, the higher strain and alteration appear to result in different sulphide mineral assemblages with higher Ni contents, discussed further below.

MINERALIZATION

The Ni–Cu (Co, PGE) mineralization in the Baikie sub-belt is hosted within, or directly associated with, thin units of talc–magnesite altered ultramafic rocks and can be subdivided into three general localities: Boomerang, Baikie and DCP, which are characterized by different mineralization styles and grades. The sulphide mineralogy observed across the sub-belt varies as a function of mineralization style (*i.e.*, disseminated, massive, vein), strain and alteration intensity.

The Baikie prospect consists of an ~11-m thick interval of blebby disseminated sulphide (2–5% sulphide minerals; Plate 4A), with two intervals (0.5- and 0.9-m thick) of massive sulphide (>95% sulphide minerals). The DCP prospect occurs ~700 m northeast along strike from the Baikie prospect and consists of a 3-m thick interval of blebby disseminated sulphide mineralization (1–3%) with 0.7% Ni reported over a cumulative 2.23 m thickness of channel samples (McLean *et al.*, 1992). The Boomerang trend to the southwest of the Baikie prospect, comprises 3 Ni prospects (Boomerang, Boomerang NE#1 and Boomerang NE#2). In contrast to the disseminated to locally massive sulphide mineralization observed at the Baikie and DCP prospects, mineralization in the Boomerang trend consists of narrow sulphide veins (~1 mm to 5 cm in diameter; Plate 4B, C) and disseminated sulphide at the contact between mafic and ultramafic rocks (Schofield and Diekrup, 2025). The best grades intercepted at the Boomerang prospect consist of 2.11% Ni over a 0.3 m long channel sample (McLean and Butler, 1993) and two drillcore intercepts of 2.25% Ni and 0.17% Cu over 0.07 m and 1.28% Ni and 0.15% Cu over 0.25 m (McLean and Butler, 1993). Similar grades and widths were intercepted at Boomerang NE#1 with 1.23% Ni, 0.05% Cu over 0.42 m and 0.83% Ni, 0.08% Cu over

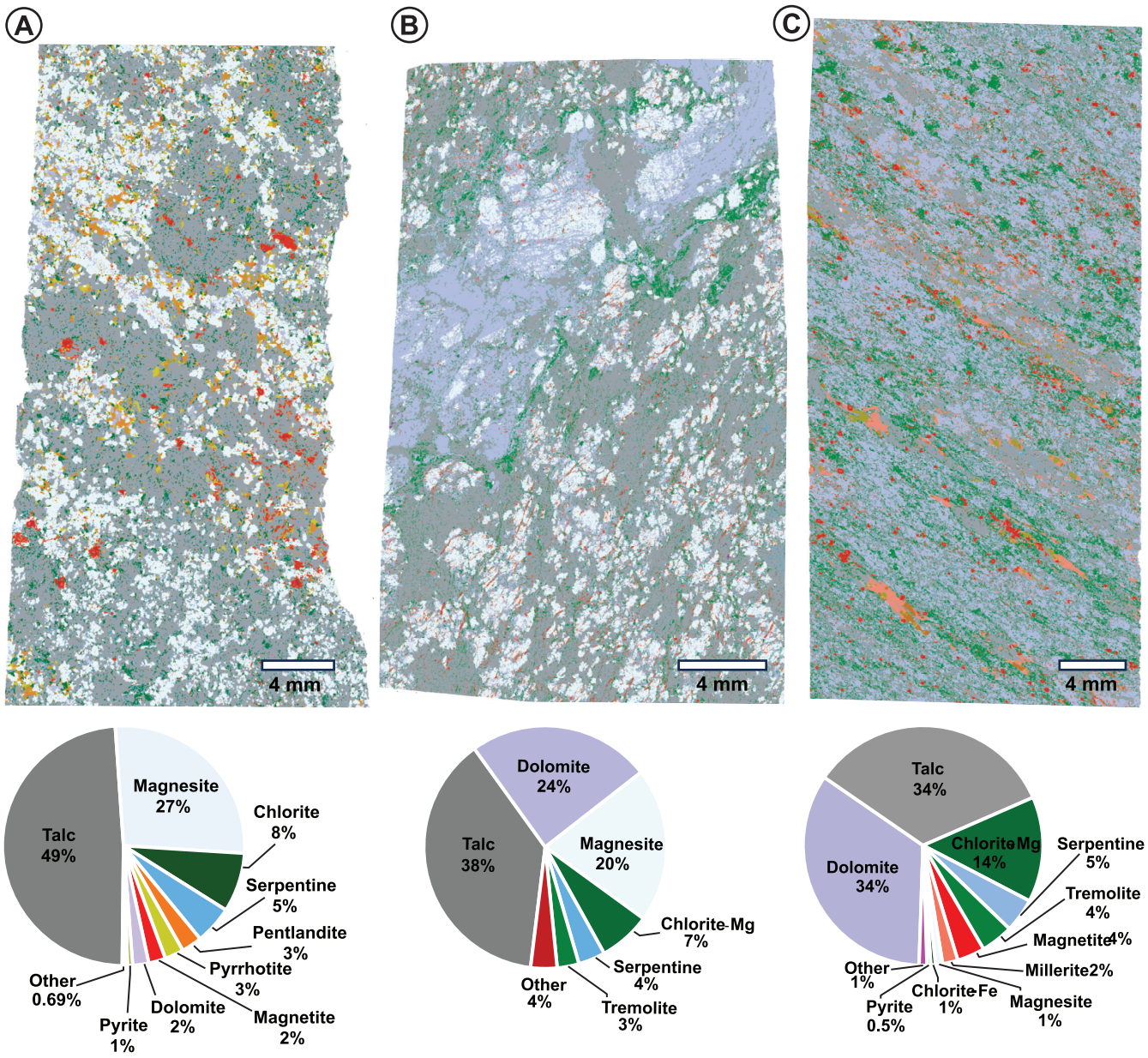

Plate 2. *False colour SEM-MLA images for thin sections from the Baikie sub-belt showing variable talc–carbonate mineral associations and overprinting relationships. Pie chart shows weight percent abundance of main mineral phases. A) Sample 24MS0001K1, Baikie prospect, talc–magnesite association, relatively undeformed; B) Sample 24MS003I1, Boomerang NE#2 prospect, incipient dolomite and chlorite alteration overprinting previous talc–magnesite association, moderately deformed; C) Sample 24MS0139E1, DCP prospect, highly deformed talc–dolomite association, showing complete replacement of magnesite and an increase in chlorite abundance.*

0.15 m (McLean and Butler, 1993). The Boomerang NE#2 prospect consists of a mineralized 0.4-m-thick sedimentary unit with 3900 ppm Ni, 754 ppm Cu and 106 ppm Co (McLean *et al.*, 1992).

In the relatively undeformed talc–carbonate-altered ultramafic samples from the Baikie prospect, the disseminated mineralization consists of irregular disseminated sulphide blebs (~0.1–2 mm diameter) of intergrown pentlandite, pyrrhotite, chalcopyrite, magnetite ± pyrite (Plates 2A and 5A). Where pyrite is present it occurs in skeletal texture with chalcopyrite, and as irregular inclusion rich bands in pyrrhotite (Plate 5B, C).

In the strongly deformed and altered samples (*e.g.*, DCP prospect; Figure 2), the sulphide intergrowths (~0.1 to

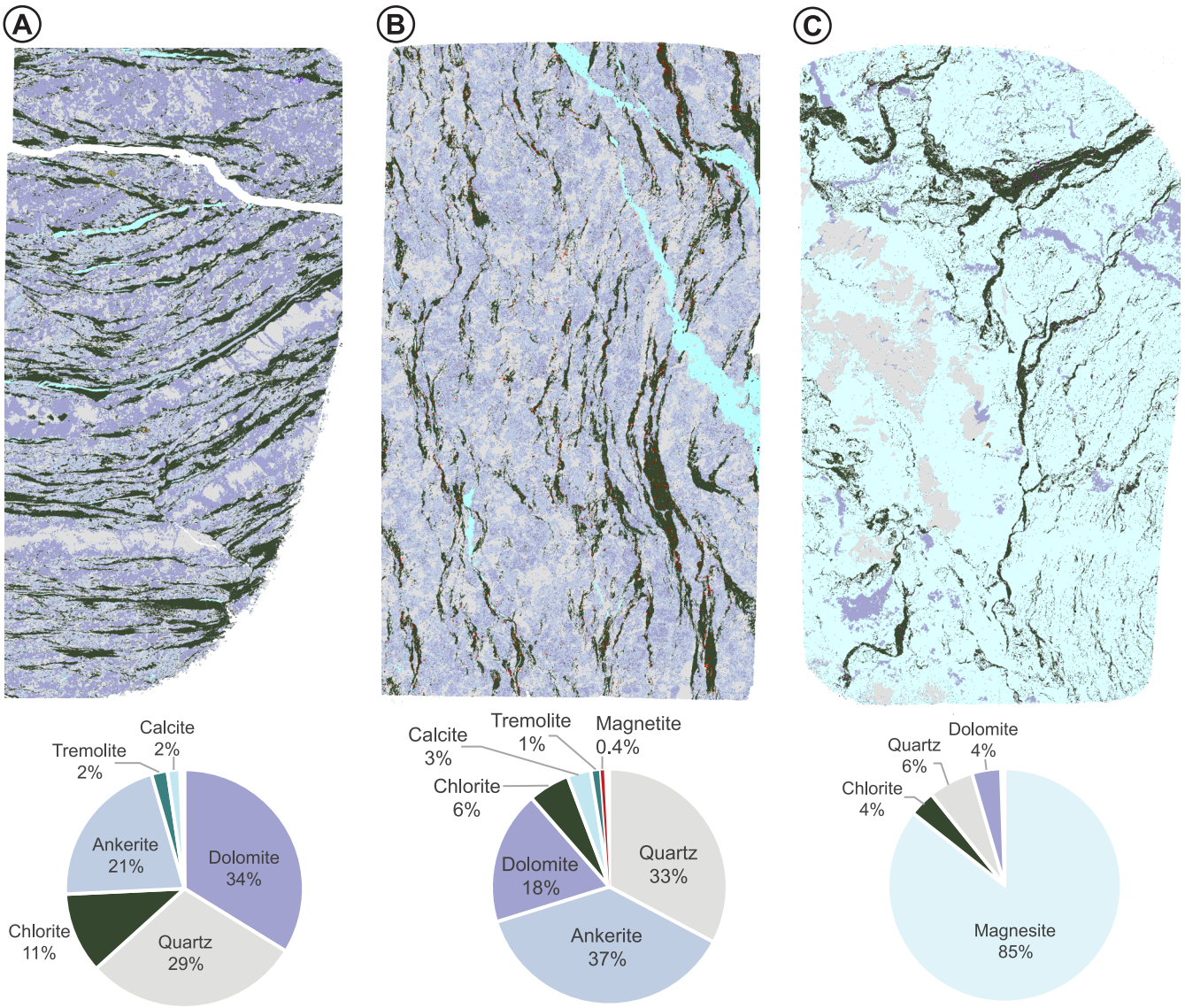

Plate 3. *False colour SEM-MLA images for quartz–carbonate altered ultramafic rocks of the Florence Lake Group. Pie chart shows weight percent abundance of main mineral phases. A) Sample 23DD0073A1, thick ultramafic unit on the northwestern margin of the Baikie sub-belt; B) Sample 22DD0129A1, Ugjoktok sub-belt; C) 23DD0068A1, Rusty Ridge, Knee Lake sub-belt.*

4 mm) are highly flattened parallel to the main pervasive foliation (Plates 2C and 5D). These sulphide intergrowths consist dominantly of millerite intergrown with siegenite (± chalcopyrite, polydymite) and euhedral ~0.1–0.2 mm diameter inclusions of pyrite (Plate 5D). Pyrrhotite is completely absent in this assemblage. The pyrite inclusions are typically rimmed by minor chalcopyrite and have a porous inclusion-rich core, inclusion-free rims, and are locally crosscut by microfractures (Plate 5E). The mineral inclusions in the pyrite consist of chalcopyrite ± tellurobismuthite ± galena ± michenerite ± hessite ± electrum (Plate 5F). Magnetite occurs as euhedral rims surrounding chromite and the grains are typically located along the margins of the sulphide blebs (Plate 5E).

The vein style mineralization at Boomerang consists dominantly of pyrrhotite and pentlandite ± chalcopyrite ± nickeliferous cobaltite. The veins are typically associated with carbonate, both as a phase within the vein and as alteration haloes (Plate 4B, C).

METHODOLOGY

All 156 samples, including 70 drillcore samples, collected from the Baikie sub-belt during the 2024 field season that were selected for geochemical analysis, were prepared at the GSNL geochemistry laboratory in St. John's. Samples were crushed using a Braun Chipmunk jaw crusher. Rock chips from the jaw crusher were then pulverized using a

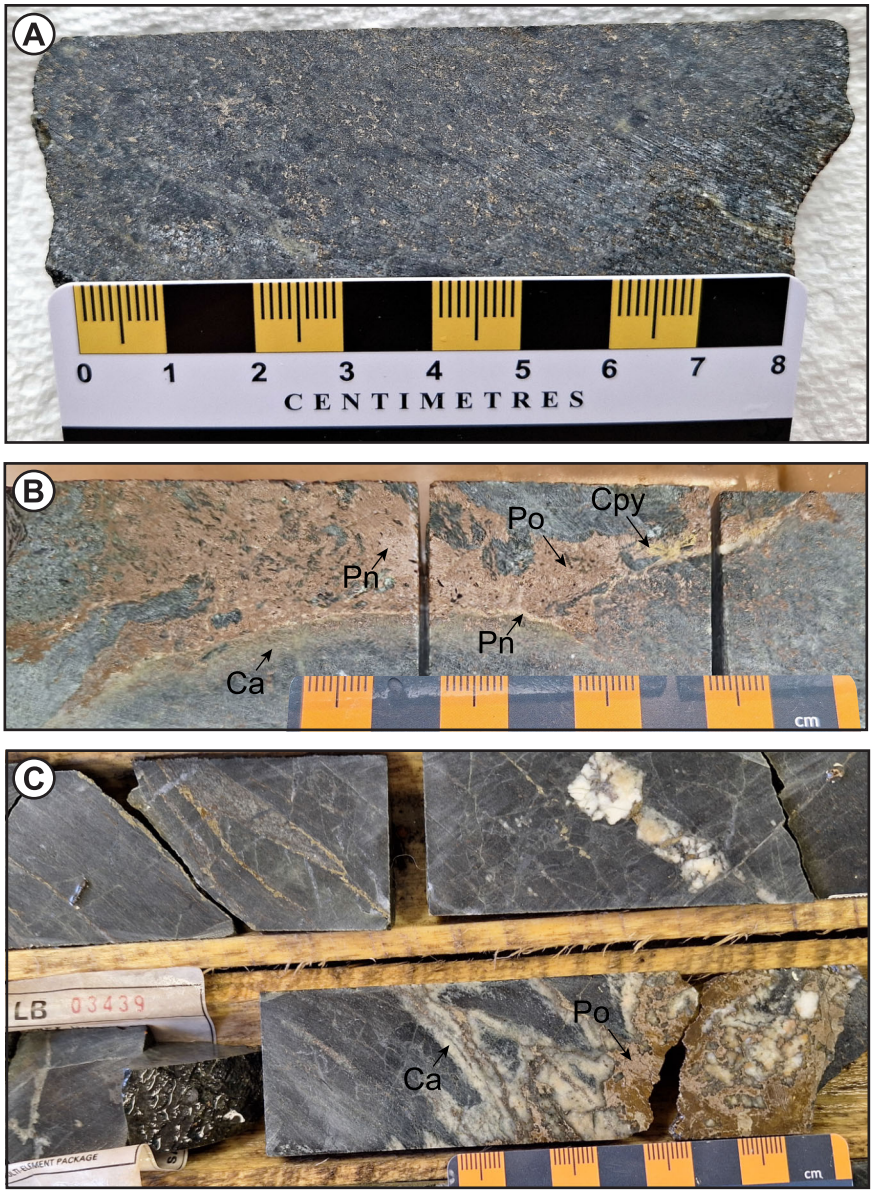

Plate 4. *Drillcore samples showing sulphide mineralization styles in the Baikie sub-belt. A) Sample of disseminated sulphide mineralization in talc–magnesite altered ultramafic rock from the main Baikie prospect. Sampled using a portable backpack drill; B) Drillcore from hole FLK-93-27 (Boomerang prospect) showing vein of pyrrhotite, pentlandite and chalcopyrite. Note, bleached calcite alteration halo; C) Drillcore from hole FLK-93-30 (Boomerang prospect) showing pyrrhotite veins associated with calcite. Ca–calcite, Cpy–chalcopyrite, Pn–pentlandite, Po–Pyrrhotite.*

T.M. Engineering mild steel ring/puck pulverizer. Standards and analytical duplicates were inserted every twenty samples. The samples were digested using a lithium tetraborate and metaborate fusion and then analyzed by ICP-OES for major-element compositions, and ICP-MS for rare-earth-elements (REE) and selected trace-element compositions. The remaining trace elements (As, Cd, Co, Cu, Li, Mo, Ni, Pb, S, V and Zn) were analyzed by ICP-OES following a 4 Acid digestion. The loss-on-ignition (LOI) was calculated after heating the sample to 1000°C.

A subset of 97 samples were sent to the ALS Canada Ltd. lab in Vancouver, BC, to analyze by the "Super-Trace, Total Extraction REE and Refractory Minerals" analytical package, which consists of an ammonium bifluoride decomposition coupled with proprietary ICP-MS technology that enables ultra-low detection limits, unachievable by traditional flux-based methods. This is particularly important for ultramafic rock compositions, which have very low concentrations of REE.

GEOCHEMISTRY RESULTS

ULTRAMAFIC GEOCHEMISTRY

Komatiites are classified as ultramafic rocks containing >18% MgO, <1% TiO_2 and <52% SiO_2 with textures or field relationships indicating a volcanic origin. Because of the highly deformed and metasomatized nature of the ultramafic rocks in the FLG, it can be difficult to ascertain a volcanic

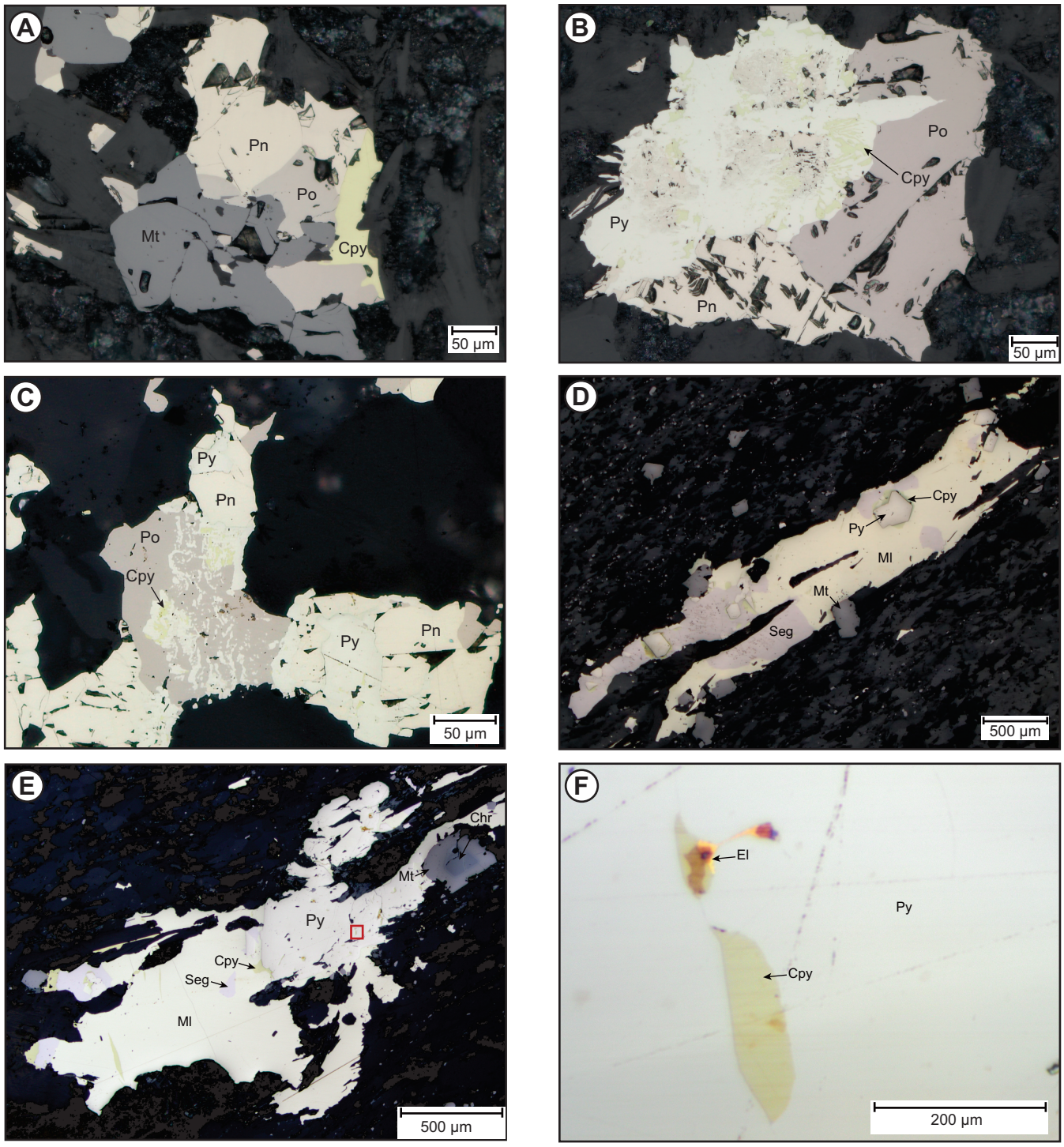

Plate 5. *Reflected light photomicrographs of sulphide mineralogy from the Baikie (A–C) and DCP (D–F) prospects. Note the change in mineralogy and textures in the relatively undeformed Baikie samples compared to the highly strained DCP sample. A) Intergrowth of pentlandite, pyrrhotite, chalcopyrite and magnetite; B) Intergrowth of pyrrhotite and pentlandite. Pyrite displays a skeletal texture with chalcopyrite and pentlandite; C) Intergrowth of pentlandite and pyrrhotite, pyrite shows skeletal texture with chalcopyrite and pyrrhotite; D) Sulphide bleb flattened parallel to foliation, consisting dominantly of intergrown millerite and siegenite. Note inclusions of euhedral recrystallized pyrite surrounded by thin rims of chalcopyrite. E) Deformed sulphide bleb showing euhedral pyrite with abundant inclusions of chalcopyrite and crosscutting microfractures. The red box highlights the location of an electrum inclusion shown in Plate 5F; F) Close-up of electrum inclusion from E. Electrum is associated with chalcopyrite and occurs along a microfracture that crosscuts the pyrite grain. Chr–chromite, Cpy–chalcopyrite, El–electrum, Mt–magnetite, MI–millerite, Pn–pentlandite, Po–pyrrhotite, Py–pyrite, Seg–siegenite.*

versus intrusive origin for all units. However, locally observed polyhedral jointing (Miller, 1996), spinifex texture (McLean and Butler, 1993), and thermal erosion features (Diekrup *et al.*, 2023), support a volcanic origin for at least some of the ultramafic units. For simplicity, all ultramafic units will be referred to as "komatiites" even for samples lacking preserved primary field relationships or textures to support a volcanic origin. In addition, some samples with <18% MgO were classified as ultramafic, because of anomalously high Ni and Cr values, and low TiO_2. Based on the MgO content, some of these might be better classified as komatiitic basalts, however, because of the mobility of MgO during alteration they were grouped with the komatiite samples for simplicity.

Komatiite compositions can be further subdivided into three main geochemical types (Al-depleted, Al-undepleted and Al-enriched or Ti-depleted) based on their Al_2O_3/TiO_2 ratios, $(Gd/Yb)_N$ and $(La/Sm)_N$ (*e.g.*, Jahn *et al.*, 1982; Kamber and Tomlinson, 2019; Waterton and Arndt, 2023). These compositional groupings reflect different degrees of partial melting, depth of melting, and/or mantle compositions and have important implications for the geodynamic evolution of greenstone belts and their potential to host magmatic Ni–Cu–Co–PGE mineralization (*e.g.*, Lesher *et al.*, 2001). The ultramafic rocks of the FLG comprise Al-undepleted and Al-depleted komatiite. The Al-depleted komatiite group has Al_2O_3/TiO_2 ratios <12 (Figure 3A) and Gd/Yb_{MN} >1.6 (Figure 3B), reflecting a relative depletion in HREE's. This is also indicated by a slightly negative slope between Gd and Lu on a primitive mantle normalized spider plot (Figure 3C). The HREE depletion suggests that garnet was present in the source residue during partial melting. In addition, the Al-depleted komatiite group is slightly enriched in REE and trace elements compared to primitive mantle (Figure 3C) and have Nb/Th_{MN} and Th/Yb_{MN} values comparable to EMORB (Figure 4). In contrast, the Al-undepleted komatiite group have Al_2O_3/TiO_2 ratios >12 (Figure 3A), Gd/Yb_{MN} <1.6 (Figure 3B) and a relatively flat REE profile

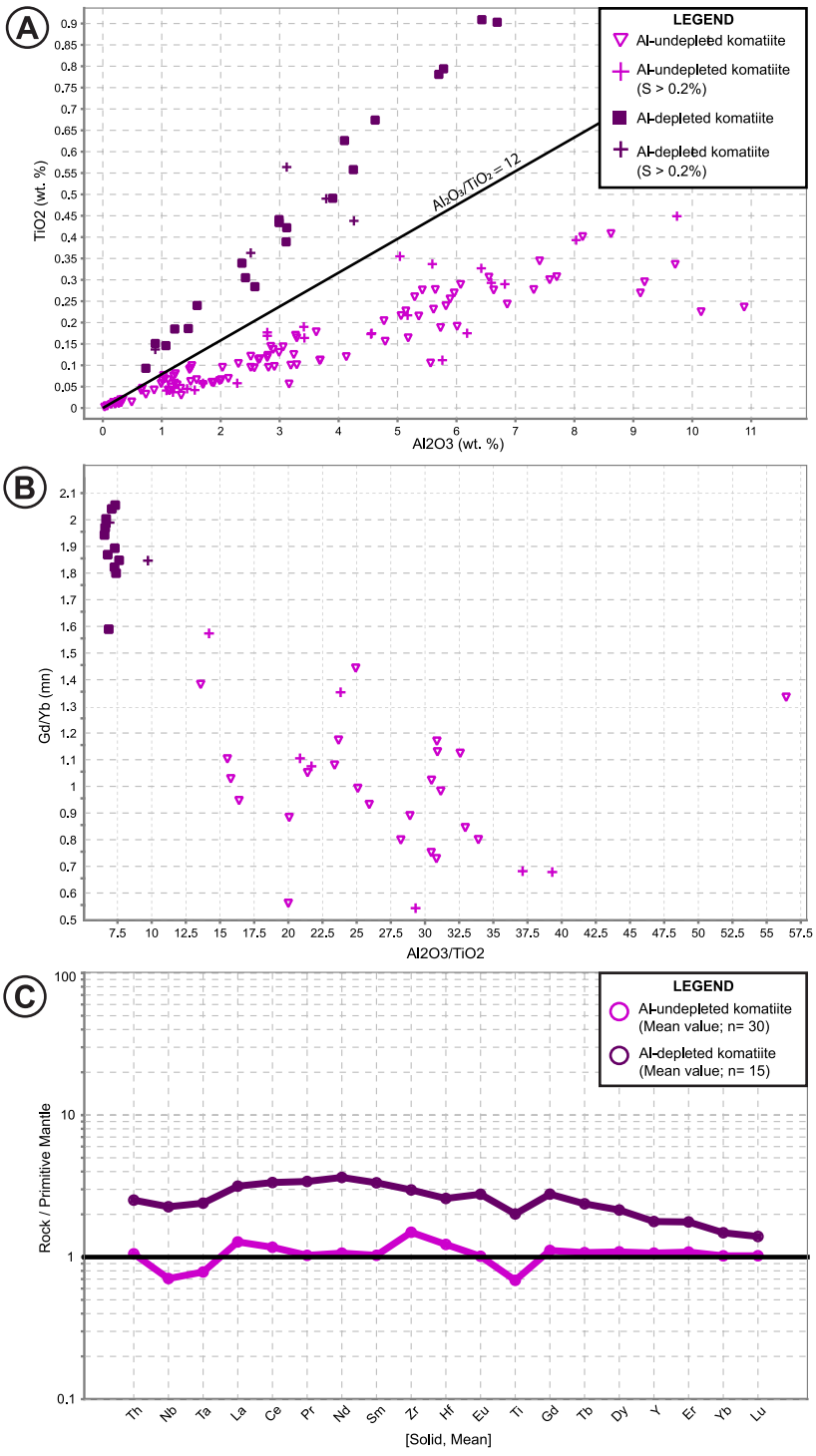

Figure 3. *Geochemical classification diagrams for ultramafic rocks of the Florence Lake Group. A) Al_2O_3* vs. *TiO_2 binary plot showing Al-depleted (Al_2O_3/TiO_2 < 12) and Al-undepleted (Al_2O_3/TiO_2 > 12) komatiite rock trends; B) Gd/Yb normalized to primitive mantle values of Sun and McDonough (1989)* vs. *Al_2O_3/TiO_2 using the subset of samples analyzed by ALS; C) Extended rare-earth element and incompatible trace-element spider plot normalized to primitive mantle values of Sun and McDonough (1989) using the subset of samples analyzed by ALS. Only mean values are shown.*

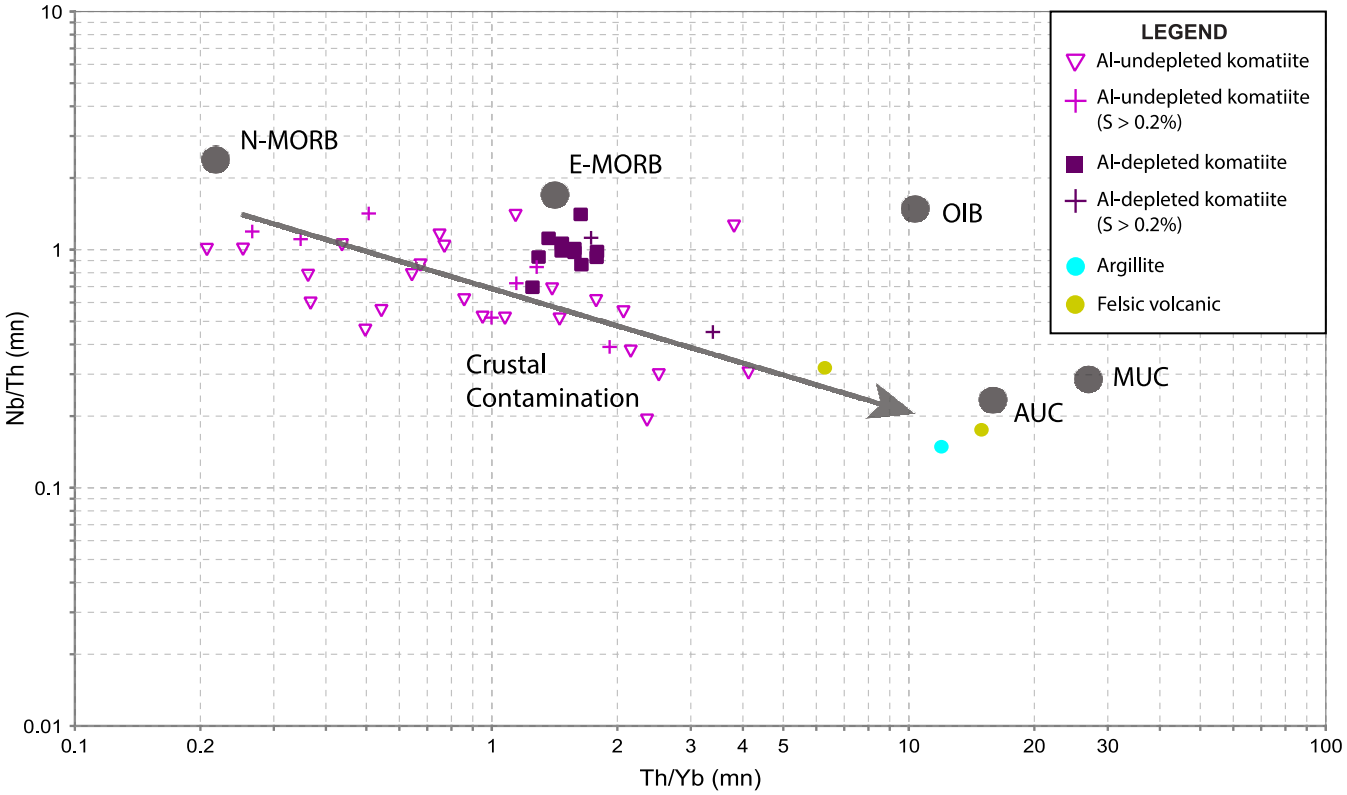

Figure 4. *Nb/Th* vs. *Th/Yb normalized to primitive mantle values of Sun and McDonough (1989) showing the effect of crustal contamination in ultramafic rocks from the Florence Lake Group (modified from Lesher* et al.*, 2001). Felsic volcanic and metasedimentary rocks from the Baikie sub-belt are also plotted for comparison. All samples shown were analyzed by ALS. AUC–Archean upper crust of Taylor and McLennan (1985), MUC–Modern upper crust of Rudnick and Fountain (1995), NMORB–normal mid-ocean-ridge basalt, EMORB–enriched mid-ocean-ridge basalt, OIB–ocean island basalt (Sun and McDonaugh, 1989).*

approximating primitive mantle values (Figure 3C). The Al-undepleted komatiite group typically has Nb/Th_{MN} <1 and Th/Yb_{MN} of 0.2–4 (Figure 4) and fall on an array between NMORB and the Archean upper crust composition of Taylor and McLennan (1985), which indicates this suite of rocks has been affected by crustal contamination. These ratios are unaffected by fractionation and accumulation of olivine, chromite and sulphide, and are assumed to be relatively consistent in mantle sources and immobile during alteration (Smithies *et al.*, 2022). Crustal contamination is further indicated by the presence of negative Nb, Ta and Ti anomalies in the Al-undepleted komatiite group (Figure 3C); the upper crust is less enriched in Ta, Nb and Ti as these elements are preferentially retained in oxide phases of eclogite during crustal recycling (*e.g.*, Weaver and Tarney, 1981; Rudnick *et al.*, 2000; Lesher *et al.*, 2001; Barnes *et al.*, 2004). In contrast, the Al-depleted komatiites cluster more tightly around EMORB with Nb/Th_{MN} ~1 and Th/Yb_{MN} 1–2 (Figure 4) and only a weak negative Ti anomaly (Figure 3C), which suggests crustal contamination is negligible for these rocks.

Other prospectivity diagrams include comparing Ni and Cr values (Brand, 1999), and Ni and MgO values (Brand, 2004) to distinguish ore-forming processes from typical magmatic processes. Mineralized komatiitic rocks typically have high Ni/Cr ratios, wherein Ni is present in both silicate and sulphide phases; barren komatiitic rocks typically have low Ni/Cr ratios indicating a higher abundance of cumulate chromite, wherein Ni is typically trapped in the silicate phase (*e.g.*, olivine; Brand, 1999). The mineralized samples from the Baikie sub-belt all follow this mineralized komatiite trend with high Ni/Cr values (Figure 5A). The samples with higher Ni/Cr ratios also typically have anomalously high Ni relative to MgO indicating a higher Ni content than can be explained by olivine fractionation, suggesting the presence of Ni sulphides (Figure 5B). Furthermore, some samples plot below the normal igneous Ni envelope suggesting they have been depleted in Ni relative to MgO, which is typically attributed to the segregation of a sulphide liquid (Brand, 2004). Olivine can accommodate both Ni and Mg into its chemical structure, so these two elements are positively correlated with lower values in more basaltic compositions and higher values in more ultramafic compositions that have higher modal abun-

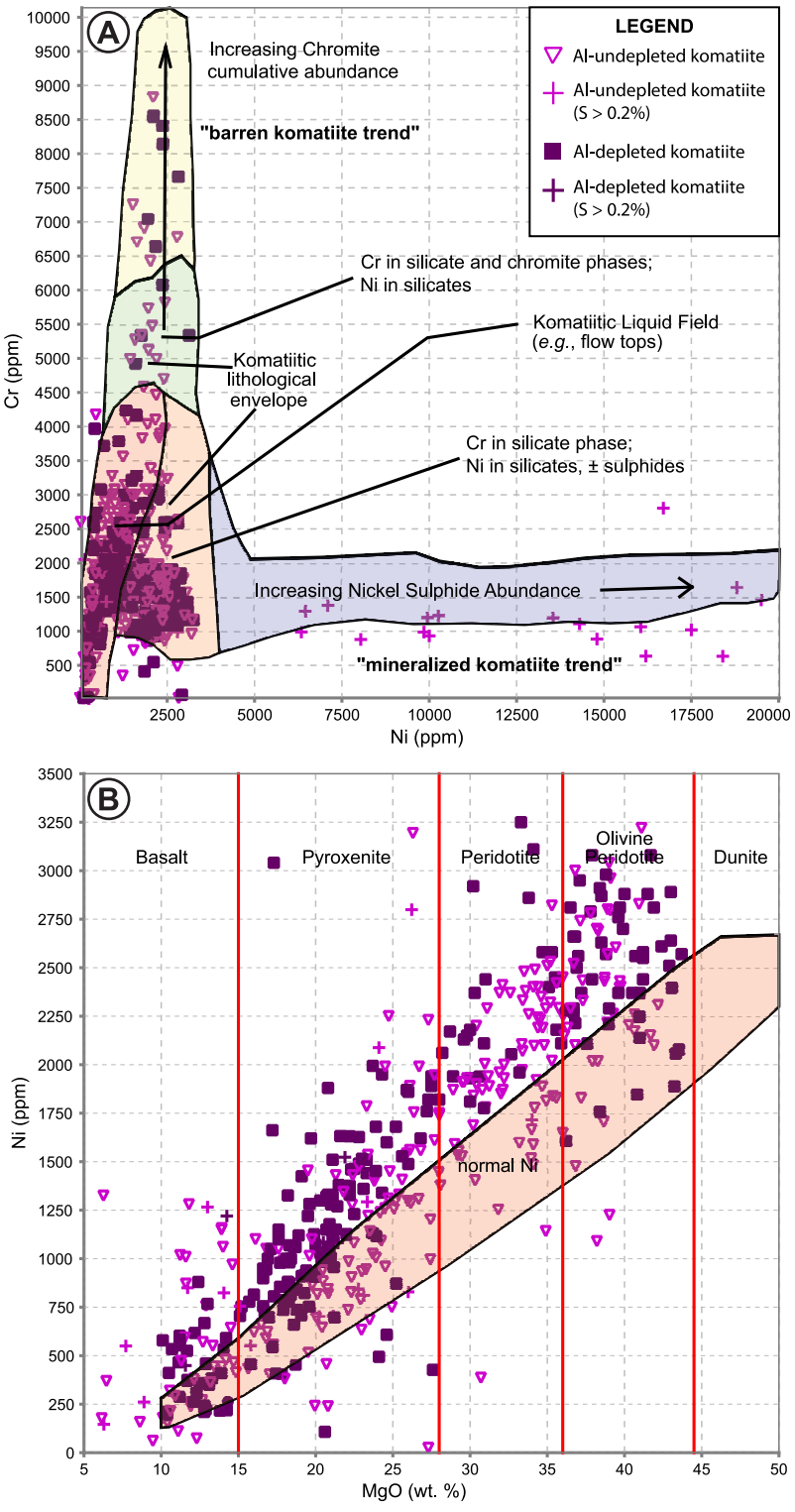

Figure 5. *Prospectivity diagrams for exploration of magmatic Ni deposits showing all ultramafic samples from the Florence Lake Group including 348 samples from Falconbridge and 81 samples from Churchill Resources. A) Ni ppm* vs. *Cr ppm (modified from Brand, 1999); B) Ni ppm* vs. *MgO wt. % (modified from Brand, 2004).*

dances of olivine ("normal Ni envelope"; Figure 5B); any deviations from this linear trend indicates the segregation and/or accumulation of Ni sulphides. However, some caution is required with this diagram as MgO can be mobile during alteration. Samples that plot above the normal Ni envelope, and contain less than 0.2% S, might have lost MgO or had their original S contents reduced by alteration.

MAFIC GEOCHEMISTRY

The basaltic rocks of the FLG fall into two compositional groups. The type 1 basalt group are characterized by broadly positively sloped REE profiles with relative depletions in Th, Nb and LREE elements (Figure 6A), which is indicated by La/Sm_{MN} <1 (Figure 6B). These are tholeiitic basalts (Figure 6C) with Th/Yb and Nb/Yb values comparable to mid-ocean ridge basalts (NMORB; Figure 6D). In addition, they have low Gd/Yb_{MN} values like the Al-undepleted komatiite group, suggesting that garnet was not present in the source residue during partial melting.

In contrast, the type 2 basalt group is more enriched in LREE and slightly depleted in HREE, exhibiting a negative-sloped REE profile (Figure 6A) and higher Gd/Yb_{MN} and La/Sm_{MN} values (Figure 6B). This group of rocks have a transitional magmatic affinity (Figure 6C) and Th/Yb and Nb/Yb values between EMORB and oceanic-arc rocks (Figure 6D), suggesting they have been crustally contaminated. This is further supported by the presence of negative Nb, Ta and Ti anomalies (Figure 6A). The western domain consists dominantly of type 1 basalt rocks. In the eastern domain, type 1 basalt rocks appear to be spatially associated with the Al-undepleted komatiite rocks and are concentrated on the southeastern margin of the Baikie sub-belt, whereas the type 2 basalt rocks appear to be associated with the Al-depleted komatiite rocks and preferentially occur to the northwest of the aforementioned group (*e.g.*, Figure 7).

DISCUSSION

The base-metal occurrences in the Baikie sub-belt are stratabound and therefore the recognition of distinct rock types and

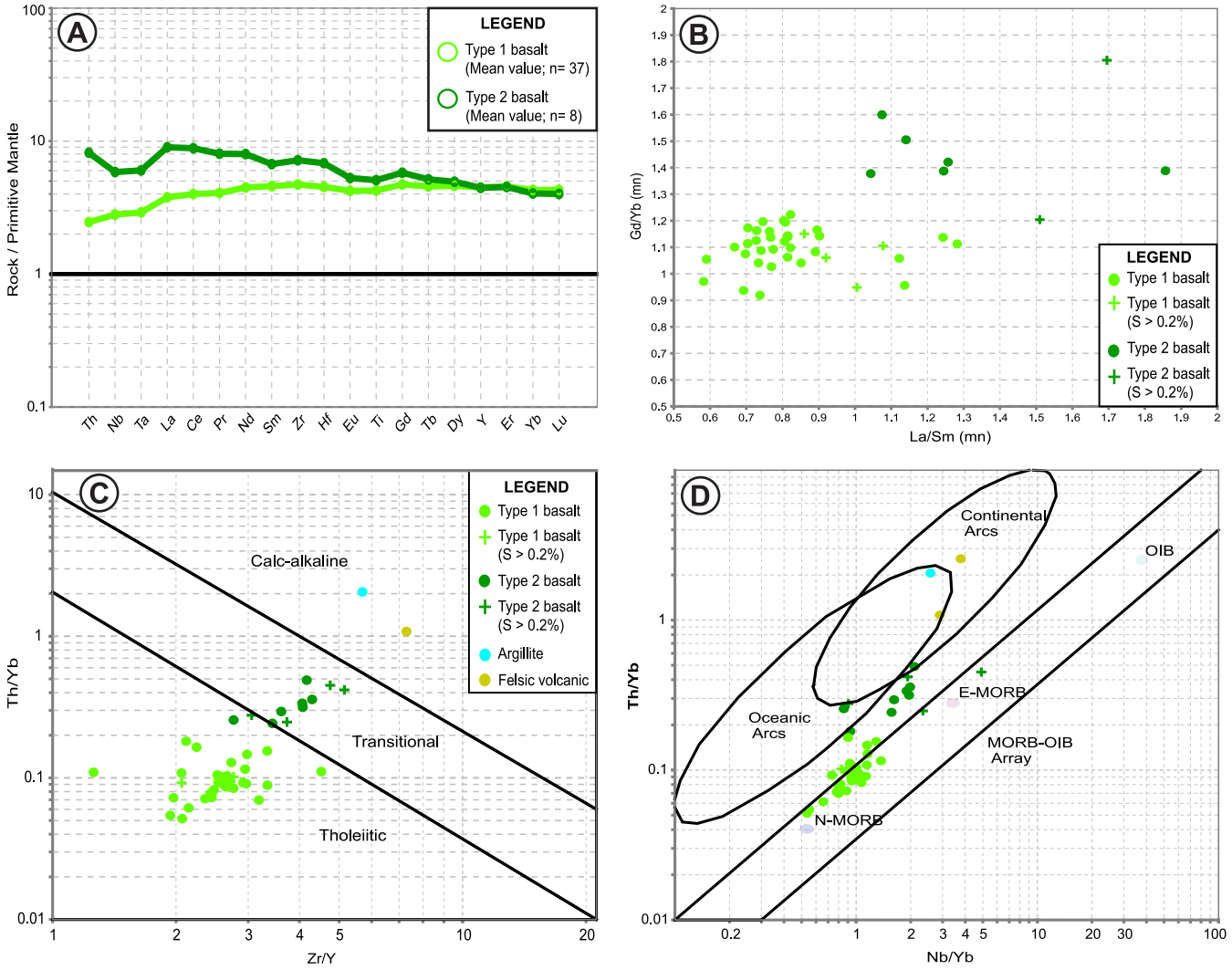

Figure 6. *Geochemical classification diagrams for mafic rocks of the Florence Lake Group using the subset of samples analyzed by ALS. A) Extended rare-earth element and incompatible trace-element spider plot normalized to primitive mantle values of Sun and McDonough (1989). Only mean values are shown; B) Gd/Yb normalized to primitive mantle values of Sun and McDonough (1989)* vs. *Al_2O_3/TiO_2; C) Magmatic affinity diagram of Ross and Bedard (2009); D) Basalt classification diagram of Pearce (2014). NMORB–normal mid-ocean-ridge basalt, EMORB–enriched mid-ocean-ridge basalt, OIB–ocean island basalt.*

facies that form markers for economically significant minerals is critical for base-metal exploration in the FLG. The new whole-rock chemistry dataset can be used to define a chemostratigraphic framework and provide insight into the geodynamic evolution of the greenstone belt and prospectivity for mineralization. The data density and outcrop exposure are much more abundant along the southeastern half (eastern domain) of the Baikie sub-belt compared to the northwestern portion (western domain; Figure 2). Therefore, any chemostratigraphic inferences for the western domain will be much less constrained than the eastern domain. Furthermore, the nature of the contact between the western domain and the eastern domain is uncertain. No conclusive younging indicators in the Baikie sub-belt have been found, however, the few younging indicators documented in the Florence Lake greenstone belt (*e.g.*, Diekrup *et al.*, 2023) suggest that the dominant younging direction is towards the southeast.

Assuming an overall southeasterly younging direction and a homoclinal sequence, the volcanic succession appears to change from a thick sequence of basaltic rocks in the western domain with one thick komatiitic unit along the westernmost margin, to intercalated basaltic, komatiitic, volcaniclastic and sedimentary rocks in the eastern domain. The basaltic rocks of the western domain are dominantly the

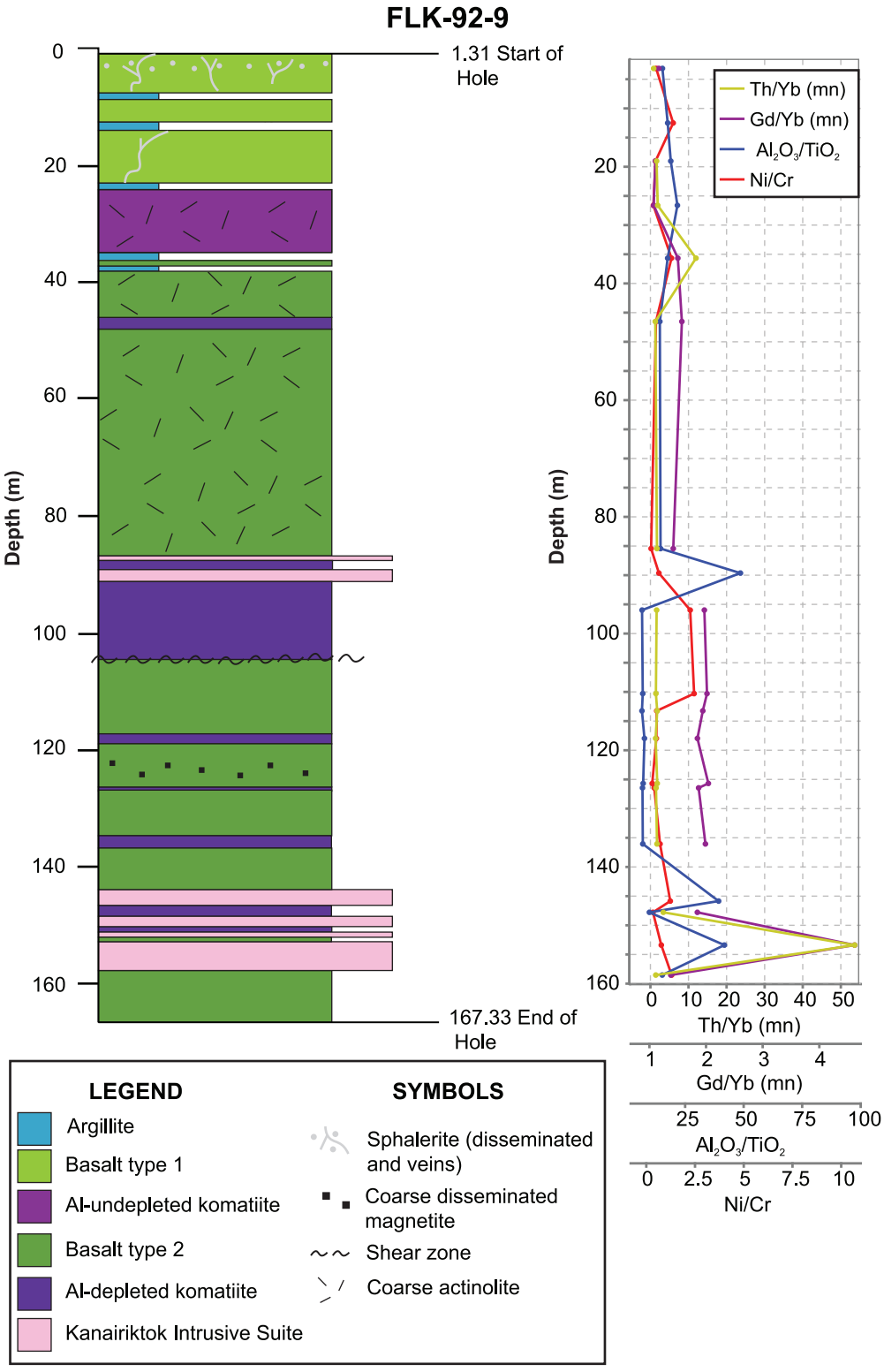

Figure 7. *Strip log for drillhole FLK-92-9, based on relogging, from the Boomerang NE#2 prospect in the Baikie sub-belt showing the spatial association between type 1 basalt and Al-undepleted komatiite rocks in the upper part of the drillhole (southeast) compared to the type 2 basalt and Al-depleted komatiite rocks that make up the lower part of the drillhole (northwest). Graph on the right shows downhole variation in select immobile incompatible element ratios used in geochemical classification diagrams shown in Figures 3–6.*

type 1 basalt composition; the basaltic rocks of the eastern domain progress from "lower" type 2 basalt, intercalated with Al-depleted komatiite, to "upper" type 1 basalt, intercalated with Al-undepleted komatiite. The thick ultramafic unit on the western margin of the western domain is of the Al-undepleted komatiite type, however, it may be intrusive and possibly related to the Al-undepleted komatiite rocks in the eastern domain. This indicates a general progression up succession in the eastern domain from more enriched and contaminated to more depleted and primitive basaltic compositions, with a concomitant change in chemistry of the ultramafic rocks from Al-depleted to Al-undepleted komatiite. All the known Ni-Cu (Co, PGE) prospects occur within the upper Al-undepleted komatiite and associated type 1 basalt units within the eastern domain. Additionally, mineralized Al-undepleted komatiite unit(s) also show evidence of crustal contamination. Komatiitic magmas are typically strongly undersaturated in sulphur when they erupt at surface; assimilation of a crustal source of sulphur, typically sulphide-bearing sedimentary units, is typically a pre-requisite to the formation of magmatic sulphide deposits. However, even though evidence of crustal contamination is important as an indicator of ore-forming processes, contamination on its own is not sufficient evidence for the prospectivity of ultramafic units to host magmatic sulphide deposits, as the crustal contaminant would also need to have sufficient sulphur to trigger sulphur saturation (Lesher *et al.*, 2001). Locally, sulphide-bearing metasedimentary units are spatially associated with the mineralized ultramafic units and might represent a crustal sulphur source for the Ni sulphide mineralization. Thus, this metasedimentary unit associated with Al-undepleted komatiite and type 1 basalts, might serve as a favourable stratigraphic marker for komatiite-hosted Ni–Cu (Co, PGE) mineralization throughout the Florence Lake greenstone belt. Pending geochronology, whole-rock geochemistry, and isotopic data will help constrain possible correlations between the sub-belts and evaluate this further.

There does not appear to be any major petrographic variation between the Al-depleted and Al-undepleted komatiitic rocks. Similarly, there does not appear to be any major petrographic variation between the two basalt groups. The presence of pillowed flows locally, indicates eruption in a submarine setting; however, the prevalence of massive flow facies in the basaltic rocks suggests relatively high effusion/eruption rates and/or relatively low viscosity magmas. The observed mineral associations in the ultramafic rocks are consistent with early seafloor hydration reactions forming serpentine and magnetite from H_2O-rich, CO_2-poor fluids followed by the formation of talc-magnesite and quartz-magnesite associations from fluids with higher CO_2. The dolomite ± ankerite and chlorite alteration appears to be a later overprint related to proximity to faults. The presence of low (<200°C) temperature hydrothermal sulphide assemblages (pyrite–millerite–chalcopyrite; *e.g.*, Holwell *et al.*, 2017) in the highly strained dolomite ± ankerite ± chlorite altered rocks, suggests that recrystallization of the primary magmatic sulphide assemblages has occurred. This process may have also locally liberated PGE's from earlier sulphide phases and introduced gold and silver.

James *et al.* (2002) proposed two possible models for the formation of the FLG: Mantle plume activity that resulted in rifting of the Maggo Gneiss basement, or a back-arc basin formed above a subduction zone, which dipped under the Maggo microcontinent. Geodynamic processes in the early Archean are highly contentious, and these two processes do not necessarily have to be mutually exclusive. However, anomalously thick and voluminous komatiite–tholeiite assemblages (*e.g.*, Stoughton-Roquemore Assemblage, Abitibi Greenstone Belt) are typically linked to mantle plume activity (*e.g.*, Thurston, 2015; Barnes *et al.*, 2016). The Al-depleted komatiite signature indicates high-pressure melts that segregated from fertile mantle sources containing residual garnet; the Al-undepleted komatiite signature indicates that the melt segregated at lower pressures, and/or from higher degrees of partial melting, where garnet was not present in the residue (Sossi *et al.*, 2016; Sproule *et al.*, 2002; Waterton and Arndt, 2023). Both komatiite types can be derived from the same mantle plume wherein Al-depleted komatiites are derived from the cooler distal fringes of the plume and the Al-undepleted komatiites are derived from the hotter central axis of the plume (Sossi *et al.*, 2016). Numerical simulations indicate that during mantle plume ascent Al-depleted komatiites are the first to be generated, under high pressures and/or low melt fractions, and upon continued decompression melting, Al-undepleted komatiites are generated (Sossi *et al.*, 2016). Other possible explanations for this shift in chemistry include a change in plume morphology with time, as it was dragged by the overlying plate, a decrease in plume ascent rate due to interaction with subducting slabs or a decrease in lithospheric thickness due to rifting (Sproule *et al.*, 2002). Regardless of the mechanism, this shift in komatiitic composition is consistent with the spatial distribution of the ultramafic units in the Baikie sub-belt assuming a southeasterly younging direction. However, the basalt chemostratigraphy in the eastern domain of the Baikie sub-belt is the reverse of what is observed in the characteristic basalt–komatiite sequences found in other greenstone belts, which typically consist of a lower low-Th tholeiitic basalt suite (*e.g.*, Lunon basalt, Kambalda) overlain by an intermediate Th basalt suite (*e.g.*, Devon Consols Basalt, Kambalda; Barnes *et al.*, 2016; Smithies *et al.*, 2022). The "low-Th" basalt suite is comparable compositionally to the type 1 basalt of this study, whereas the "intermediate-Th" basalt suite is comparable to the type 2 basalt, which occurs to the northwest or stratigraphically below the type 1 basalt in the eastern domain of

the Baikie sub-belt. In the Kambalda domain of the Kalgoorlie terrane the mineralized Al-undepleted komatiite unit occurs at the contact between these two basalt types (Barnes *et al.*, 2016), which also appears to be the case in the Baikie sub-belt. The low-Th tholeiitic basalts at Kambalda, which are the most voluminous, were interpreted to be the Archean analogue of plume-head large igneous province basalts, similar to Phanerozoic oceanic plateau basalts (Barnes *et al.*, 2016). The intermediate Th basalts were interpreted to be derived from higher degrees of partial melting, based on higher MgO contents, but with higher degrees of contamination indicated by relatively high incompatible trace element concentrations (Smithies *et al.*, 2022). The overall increase in degree of crustal contamination and fractional crystallization signatures with time in the Kambalda area were interpreted to reflect a decrease in extension and thickening of the crust resulting in more magma ponding (Smithies *et al.,* 2022). There does not appear to be any major difference in the MgO content between the two basalt types in the Baikie sub-belt, and the lower basalt units in the eastern domain appear to be more crustally contaminated than the upper units. The basalt chemistry in the eastern domain of the Baikie sub-belt might indicate a local northwesterly younging direction, or a slightly different geodynamic setting or process than what formed the volcanic sequence in the Kambalda domain. Further data is required to evaluate this and better understand the emplacement of the FLG and other supracrustal outliers within the Hopedale Block and this is part of ongoing research (*e.g.*, Diekrup *et al.*, 2024).

CONCLUSIONS

The Baikie sub-belt of the Florence Lake Group consists of a western domain of dominantly depleted basalt (type 1 basalt) and an eastern domain with a lower sequence of enriched basalt (type 2 basalt) and Al-depleted komatiite and an upper sequence of depleted basalt (type 1 basalt) and Al-undepleted komatiite. The Ni- prospects in the Baikie sub-belt are all hosted by the upper Al-undepleted komatiite and locally type 1 basalt rocks. The mineralized komatiitic rocks show evidence for crustal contamination including negative Nb, Ta and Ti anomalies and enrichment in highly incompatible lithophile elements. In addition, the mineralized samples typically have anomalously high Ni/Cr and Ni/MgO relative to normal igneous values, reflecting the presence of Ni sulphides. These criteria can be used to look for comparable sequences and evidence of similar ore-forming processes in the other sub-belts of the FLG.

Furthermore, the sulphide mineralogy varies as a function of strain and alteration intensity ranging from relatively undeformed sulphide blebs with intergrown pyrrhotite, pentlandite and chalcopyrite ± pyrite to highly flattened sulphide blebs with intergrown siegenite, millerite, polydymite, and chalcopyrite with recrystallized euhedral pyrite. The observation of inclusions of chalcopyrite ± tellurobismuthite ± galena ± michenerite ± hessite ± electrum within the recrystallized pyrite suggests liberation of PGM from other phases during deformation and alteration as well as possible introduction of gold and silver from orogenic fluids. In addition, the change from pentlandite to more Ni-rich phases (millerite, polydymite) in the more strained and altered Ni-prospects could have important metallurgical implications.

ACKNOWLEDGMENTS

Fieldwork was supported by GSNL colleague Ludovico Scorsolini. Field assistants Sadman Rahman, Aspen Hosson and Sophia Wheeler are thanked for their eager and able assistance in the field. The authors extend great appreciation to the Aqvituk (Hopedale) community members for their hospitality and contributions to the success of this project. Helicopter support was provided by Helicopters Canada, through pilot Hayden Ramer. Justin Emberley is thanked for his assistance with the Goose Bay Core Storage Facility. Dylan Goudie is thanked for his assistance with MLA mapping. Paul Sobie of Churchill Resources Inc. is thanked for providing digitized legacy data. The manuscript was improved by helpful review by James Conliffe and Hamish Sandeman.

REFERENCES

Barnes, S.J., Hill, R.E.T., Perring, C.S. and Dowling, S.E.
2004: Lithogeochemical exploration for komatiite-associated Ni-sulfide deposits: strategies and limitations. Mineralogy and Petrology, Volume 82, pages 259-293.

Barnes, S.J., Mole, D.R., Wyche, S. and Dering, G.
2016: Komatiites and associated rocks of the Kalgoorlie-Leonora region. Geological Survey of Western Australia, Record 2016/12, 70 pages.

Brace, T.D. and Wilton, D.H.C.
1990: Platinum-group elements in the Archean Florence Lake Group, central Labrador. Canadian Mineralogist, Volume 28, pages 419-429.

Brand, N.W.
1999: Element ratios in nickel sulphide exploration: vectoring towards ore environments. Journal of Geochemical Exploration, Volume 67, pages 145-165.

2004: Geochemical expressions of nickel sulphide deposits. AIG Seminar, Advances and Innovations in the Exploration for Nickel Sulphide Deposits, Perth WA, 12 November 2004.

Bridgewater, D., Watson, J. and Windley, B.F.
1973: The Archean craton of the North Atlantic region. Philosophical Transactions of the Royal Society of London, Series A, Volume 273, pages 493-512.

Cullen, M.P. and Churchill, R.A.
1997: Sixth year assessment report on 1996 prospecting, mapping, soil sampling, grid rehabilitation and diamond drilling for licenses 376M, 378M, 396M, and 4454M; Florence Lake area, East Central Labrador NTS Sheets 13K/10 & 13K/15. Newfoundland and Labrador Geological Survey, Assessment File 013K/0231, 224 pages.

Diekrup, D., Hinchey, A.M., Campbell, H.E., Rayner, N. and Piercey, S.J.
2023: Stratigraphy, structure and mineral potential of the 3.0 Ga Florence Lake greenstone belt, Labrador. *In* Current Research. Government of Newfoundland and Labrador, Department of Industry, Energy and Technology, Geological Survey, Report 23-1, pages 151-161.

Diekrup, D., Hinchey, A.M., Mendoza Marin, D. and Sandeman, H.A.I.
2024: Structural control on the emplacement of the Florence Lake Group and adjacent supracrustal outliers in the southeastern Hopedale Block, Labrador. *In* Current Research. Government of Newfoundland and Labrador, Department of Industry, Energy and Technology, Geological Survey, Report 24-1, pages 143-154.

Dubé, B. and Mercier-Langevin, P.
2020: Gold deposits of the Archean Abitibi Greenstone belt, Canada. *In* Geology of the World's Major Gold Deposits and Provinces. *Edited by* R.H. Sillitoe, R.J. Goldfard, F. Robert and S.F. Simmons. Society of Exploration Geophysicists. Special Publication, pages 669-708.

Dunsworth, S. and Moss, R.
2026: Technical report on the Hopedale Gold Project, north central Labrador, Newfoundland and Labrador. Labrador Gold Corp., NI 43-101 report, 114 pages.

Einaudi, M.T., Hedenquist, J.W. and Inan, E.E.
2003: Sulfidation state of fluids in active and extinct hydrothermal systems: Transitions from porphyry to epithermal environments. Society of Exploration Geophysicists, Special Publication, pages 285-314.

Ermanovics, I.F.
1993: Geology of the Hopedale Block, southern Nain Province, and the adjacent Proterozoic terranes, Labrador, Newfoundland. Geological Survey of Canada, Memoir 431, 172 pages.
https://doi.org/10.4095/183986

Evans-Lamswood, D. and Sobie, P.
2022: Eight year assessment report for map staked license 027520M & first year assesmment report for map-staked licenses 032167M, 032231M & 033881M, on airborne geophysical surveys and due-diligence sampling on the Florence Lake property, Labrador NTS sheet 13K/15. Newfoundland and Labrador Geological Survey, Assessment File 013K/0362, 72 pages.

Fiorentini, M., Beresford, S., Barley, M., Duuring, P., Bekker, A., Rosengren, N., Cas, R. and Hronsky, J.
2012: District to camp controls on the genesis of komatiite-hosted nickel sulfide deposits, Agnew-Wiluna Greenstone belt, Western Australia: Insights from the Multiple Sulfur Isotopes. Economic Geology, Volume 107, pages 781-796.

Fisher, R.V. and Schmincke, H.U.
1984: Pyroclastic Rocks. Springer, Berlin Heidelberg, Berlin, Heidelberg.
https://doi.org/10.1007/978-3-642-74864-6

Hinchey, A.M., Rayner, N., Diekrup, D., Sandeman, H.A.I. and Mendoza Marin, D.
2024: New U–Pb SHRIMP age constraints on the geodynamic evolution of the Hopedale Block, Labrador: Implications for the assembly of the North Atlantic Craton. *In* Current Research. Government of Newfoundland and Labrador, Department of Industry, Energy and Technology, Geological Survey, Report 24-1, pages 155-180.

Holwell, D.A., Adeyemi, Z., Ward, L.A., Smith, D.J., Graham, S.D., McDonald, I. and Smith, J.W.
2017: Low temperature alteration of magmatic Ni-Cu-PGE sulfides as a source for hydrothermal Ni and PGE ores: A quantitative approach using automated mineralogy. Ore Geology Reviews, Volume 91, pages 718-740.

Jahn, B.M., Gruau, G. and Glikson, A.Y.
1982: Komatiites of the Onverwacht Group, S. Africa: REE geochemistry, Sm/Nd age and mantle evolution. Contributions to Mineralogy and Petrology, Volume 80, pages 25-40.

James, D.T., Kamo, S. and Krogh, T.
2002: Evolution of 3.1 and 3.0 Ga volcanic belts and a new thermotectonic model for the Hopedale Block, North Atlantic craton (Canada). Canadian Journal of Earth Sciences, Volume 39(5), pages 687-710.

James, D.T., Miller, R.R., Patey, R. P., Thibodeau, S. and Kilfoil, G.J.
1996: Geology and mineral potential of the Archean Florence Lake greenstone belt, Hopedale block (Nain Province), eastern Labrador. *In* Current Research. Government of Newfoundland and Labrador, Department of Natural Resources, Geological Survey, Report 96-1, pages 85-107.

Kamber, B.S. and Tomlinson, E.L.
2019: Petrological, mineralogical and geochemical peculiarities of Archaean cratons. Chemical Geology, Volume 511, pages 123-151.

Lesher, C.M., Burnham, O.M., Keays, R.R., Barnes, S.J. and Hulbert, L.
2001: Trace-element geochemistry and petrogenesis of barren and ore-associated komatiites. The Canadian Mineralogist, Volume 39, pages 673-696.

McLean, S. and Butler, D.
1993: Report on geological surveys, geochemical surveys, geophysical surveys and diamond drilling on mapped staked licences 377M, 403M, 461M, 463M, 576M and 578M held by Falconbridge limited. Newfoundland and Labrador Geological Survey, Assessment File 013K/15/0200, 624 pages.

McLean, S., Butler, D. and Osmond, R.
1992: Report on geological surveys, geophysical surveys and diamond drilling on mapped staked licenses 377M, 403M, 456M and 457M held by Falconbridge. Newfoundland and Labrador Geological Survey, Assessment File 013K/15/0189, 380 pages.

Miller, R.R.
1996: Ultramafic rocks and Ni–Cu mineralization in the Florence Lake–Ugjoktok Bay area, Labrador. *In* Current Research. Government of Newfoundland and Labrador, Department of Natural Resources, Geological Survey, Report 96-1, pages 163-173.

Miller, R.R. and James, D.T.
1997: Geology of the northwestern part of the Florence Lake greenstone belt and the Baikie showing, Hopedale Block (Nain Province), eastern Labrador (western part of NTS area 13K/15). Government of Newfoundland and Labrador, Department of Mines and Energy, Geological Survey, Map 97-02, Scale 1:25 000.

Pearce, J.A.
2014: Immobile element fingerprinting of ophiolites. Elements, Volume 10, pages 101-108.

Ross, P.S. and Bedard, J.H.
2009: Magmatic affinity of modern and ancient subalkaline volcanic rocks determined from trace-element discriminant diagrams. Canadian Journal of Earth Sciences, Volume 46, pages 823-839.

Rudnick, R.L., Barth, M.G., Horn, I. and McDonough, W.F.
2000: Rutile-bearing refractory eclogites: Missing link between continents and depleted mantle. Science, Volume 287, pages 278-281.
https://doi.org/10.1126/science.287.5451.278

Rudnick, R.L. and Fountain, D.M.
1995: Nature and composition of the continental crust: A lower crustal perspective. Reviews of Geophysics. Volume 33, pages 267-309.

Sandeman, H.A.I., Hinchey, A.M., Diekrup, D. and Campbell, H.E.
2023: Lithogeochemical and Nd isotopic data for Hunt River belt and Weekes amphibolite, Hopedale Block, Labrador: Evidence for two stages of mafic magmatism at >3200 Ma and ~3100 Ma. *In* Current Research. Government of Newfoundland and Labrador, Department of Industry, Energy and Technology, Geological Survey, Report 23-1, pages 77-98.

Schofield, M. and Diekrup, D.
2025: Preliminary Investigations into the distribution of magmatic Ni–Cu–PGE mineralization in ultramafic–mafic rocks of the Florence Lake Group, Hopedale Block, Labrador. *In* Current Research. Government of Newfoundland and Labrador, Department of Industry, Energy and Technology, Geological Survey, Report 25-1, pages 63-78.

Smithies, R.H., Lowrey, J.R., Sapkota, J., De Paoli, M.C., Hayman, P., Barnes, S.J., Champion, D.C., Masurel, Q., Thebaud, N., Grech, L.L., Drummond, M. and Maas, R.
2022: Geochemical characterization of the magmatic stratigraphy of the Kalgoorlie and Black Flag Groups – Ora Banda to Kambalda Region. Geological Survey of Western Australia, Report 226, 108 pages.

Sossi, P.A., Eggins, S.M., Nesbitt, R.W., Nebel, O., Hergt, J.M., Campbell, I.H., O'Neill, H, Van Kranendonk, M. and Davies, D.R.
2016: Petrogenesis and geochemistry of Archean Komatiites. Journal of Petrology, pages 1-38.

Sproule, R.A., Lesher, C.M., Ayer, J.A., Thurston, P.C. and Herzberg, C.T.
2002: Spatial and temporal variations in the geochemistry of komatiites and komatiitic basalts in the Abitibi

greenstone belt. Precambrian Research, Volume 115, pages 153-186.

Sun, S.S. and McDonough, W.F.
1989: Chemical and isotopic systematics of oceanic basalts: Implications for mantle composition and processes. Geological Society, London, Special Publications, Volume 42, pages 313-345.

Taylor, S.R. and McLennan, S.M.
1985: The Continental Crust: Its composition and Evolution. Blackwell Scientific, London, U.K.

Thurston, P.C.
2015. Igneous Rock Associations 19. Greenstone Belts and Granite−Greenstone Terranes: Constraints on the nature of the Archean World. Geoscience Canada, Volume 42, pages 437-484.
https://doi.org/10.12789/geocanj.2015.42.081

Wardle, R.J., Gower, C.F., Ryan, B., Nunn, G.A.G., James, J.T. and Kerr, A.
1997: Geological Map of Labrador; 1:1 million scale. Government of Newfoundland and Labrador, Department of Mines and Energy, Geological Survey, Map 97-07.

Waterton, P. and Arndt, N.
2023: Komatiites: their geochemistry and origins. *In* The Archean Earth: Tempos and Events (2nd Edition of the Precambrian Earth). *Edited by* M. Homann and oth-*ers*. Elsevier. https:/doi.org/10.31223/X5PX0X

Weaver, B.L. and Tarney, J.
1981: The Scourie dyke suite: Petrogenesis and geochemical nature of the Proterozoic sub-continental mantle. Contributions to Mineralogy and Petrology, Volume 78, pages 175-188.